Radiation Physics and Chemistry 125 (2016) 220–226

Contents lists available at ScienceDirect

Radiation Physics and Chemistry

journal homepage: www.elsevier.com/locate/radphyschem

Improved radiation resistant properties of electron irradiated c-Si solar cells

Khuram Ali [a,b,*], Sohail A. Khan [a], M.Z. MatJafri [a]

[a] Nano-Optoelectronics Research and Technology Laboratory, School of Physics, Universiti Sains Malaysia, Penang 11800, Malaysia
[b] Department of Physics, University of Agriculture, Faisalabad 38040, Pakistan

HIGHLIGHTS

- c-Si solar cells were fabricated and subjected to 9 MeV electron radiation.
- I-V measurements of pre and post irradiated and annealed solar cells.
- Capacitance and conductance characteristics were done before and after irradiation.
- Increase in density of interface states and trap time constant after irradiation.
- FSP solar cell showed lower degradation and higher efficiency recovery ratios.

ARTICLE INFO

Article history:
Received 31 October 2015
Received in revised form
20 April 2016
Accepted 21 April 2016
Available online 23 April 2016

Keywords:
Solar cell
Irradiation
Defects
Annealing
Capacitance-conductance

ABSTRACT

This work investigates the radiation tolerance of c-Si solar cells under electron energy of 9 MeV with fluence of 5.09×1016 cm^{-2} The solar cells were fabricated and characterized before and after electron irradiation through current-voltage (*I-V*), capacitance-voltage (*C-V*), and frequency dependent conductance (G_p) measurements. The results revealed that all the output parameters such as short circuit current (I_{sc}), open circuit voltage (V_{oc}), series resistance (R_s), and efficiency (η) were degraded after electron irradiation. Capacitance-Voltage measurements show that there is a slight decrease in the base carrier concentration (N_D), while a small increase in depletion layer width (W_D) was due to an increase in the base carrier concentration. Enhancements in the density of interface states (N_{ss}), and trap time constant (τ) have been observed after electron irradiation. The results has revealed that back surface field (BSF) solar cell with front surface passivation (FSP) presented lowest efficiency degradation ratio of 11.3% as compared to 15.3% of the solar cell without FSP. The subsequent annealing of irradiated Si solar cell devices revealed that the Si solar cell with FSP demonstrated high efficiency recovery ratio of 94% as compared to non-FSP solar cell.

1. Introduction

Solar cells are highly sensitive to radiation environment, especially in the presence of charged particles (electrons/protons etc.) (HU, 2006). Radiation of this type are abundantly available in space that cannot be avoided and are widely used to study ionization/displacement damage effects in the devices (Srour et al., 2003). Lattice defects in semiconductor devices are the outcome of exposure to these types of high-energy radiation. Such defects are responsible for decreasing the output power of the solar cells (Yamaguchi, 2001; Ali et al., 2013). Additional energy levels in the band gap are the ultimate result of the changes caused by charged particles in the lattice periodicity. These new energy levels or defect centres vary the electrical characteristics of solar cells (Sathyanarayana Bhat et al., 2015).

These radiation induced defect centres reduce the base carrier concentration, increase the series resistance and broaden the depletion layer width (Sathyanarayana Bhat et al., 2014). Usually, one to two displacements with an introductory rate of the order of 1 cm^{-1} are produced due to electrons in the range of 0.1 to several MeV (Corbett, 1966). On the average, a fluence of 10^{16} cm^{-2} is important to create a homogeneous distribution of displacements with 10^{16} cm^{-3} concentrations (Bourgoin and De Angelis, 2001). Capacitance-voltage (*C-V*) curves provide the important information about the carrier concentration, built-in voltage and the depletion layer widths of the solar cells (Rao et al., 2009). One of the most reliable and commonly adopted interface trap density (N_{ss}) extraction technique is the conductance method which is used to

* Corresponding author.
E-mail address: khuram_uaf@yahoo.com (K. Ali).

http://dx.doi.org/10.1016/j.radphyschem.2016.04.015
0969-806X/

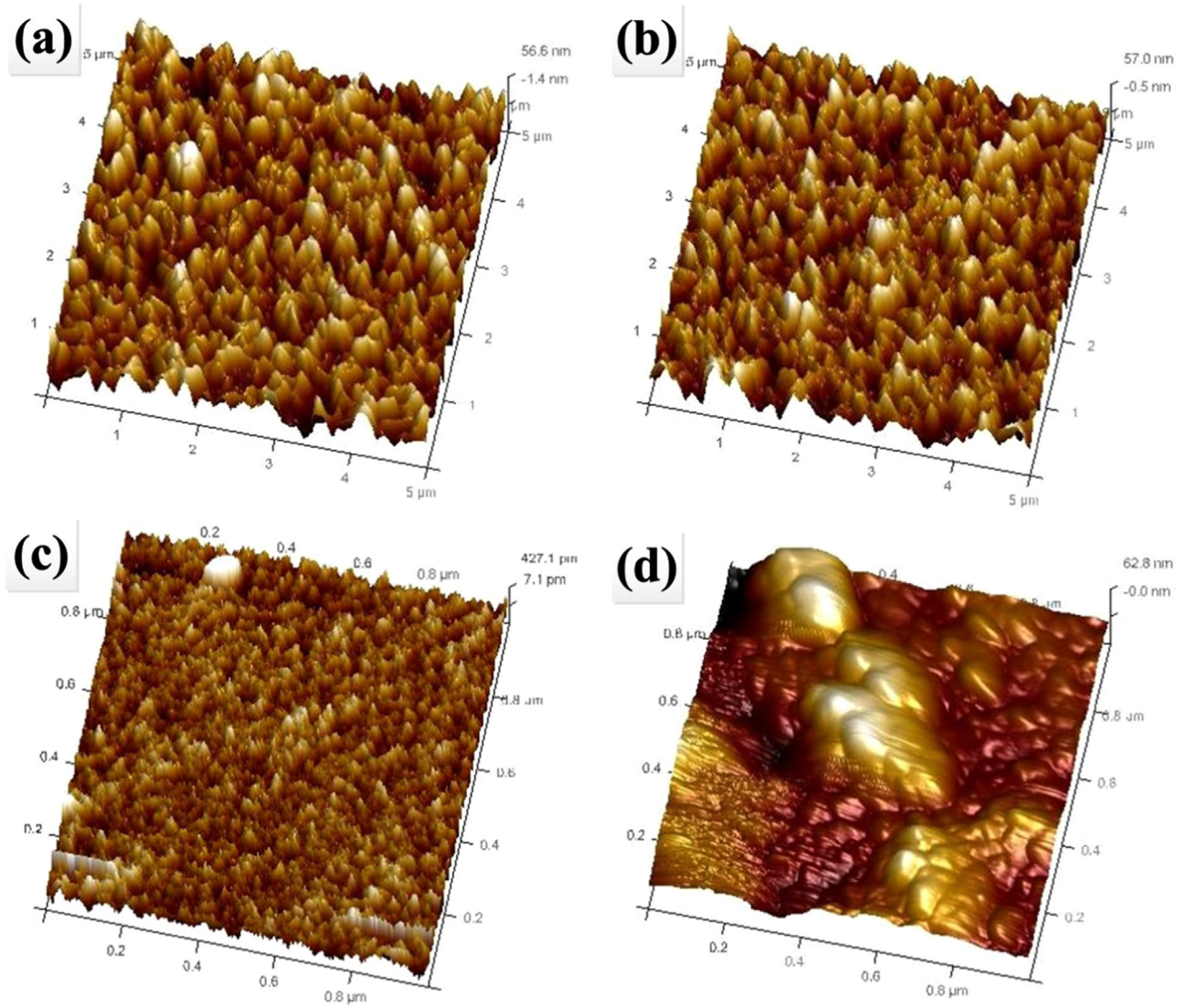

Fig. 1. AFM images of (a) SiO_2 as AR coating for solar cell with FSP, (b) SiO_2 as AR coating for solar cell without FSP, (c) as grown silicon and (d) Al alloying BSF.

evaluate the passivation of interfaces (Nicollian and Brews, 1982). This technique involves the measurement of an equivalent parallel conductance of the solar cell as a function of frequency. This method involves the loss mechanism produced by the capture and emission of carriers from the interface traps and can be used to extract the interface state density (Kao et al., 2010).

The initial efficiency of irradiated solar cell can be restored by annealing the solar cell for various time duration depending on the radiation fluence and radiation resistant properties of solar cell (Khan et al., 2002a; Kuendig and Shah, 2002). Annealing process involves the passivation of the irradiation induced defects of the solar cell with the annealing temperatures ranging from room temperature to 475 °C (Kawasuso et al., 1995; Yamaguchi et al., 1984).

In the present research work radiation tolerance of silicon cells was characterized using 9 MeV electron irradiation of 5.09×10^{16} e/cm^2. Changes in the electrical performance, *C–V* and frequency dependent conductance measurements as well as recovery of the solar cells under thermal annealing are presented in this paper.

2. Experimental techniques

The solar cells were fabricated using boron-doped p-type (100) oriented Si wafers with a size of 2×2 cm^2 and thickness of 100 μm. After RCA clean the p-n junction was realized by performing the thermal diffusion of the phosphorous atoms in a quartz tube furnace at 1000 °C. Phosphosilicate glass (PSG) formed in the diffusion process was then removed by using 1:50 HF: H_2O. The samples were then rinsed with deionized (DI) water of high purity ($\rho > 18.2$ MΩcm). Back surface field (BSF) was formed by 3 μm thick layer of high-purity aluminum (99.999%). Aluminum layer was thermally evaporated on the entire back surface and then annealed at 850 °C, followed by SiO_2 antireflection coatings. One sample was thermally passivized on the front surface while the other remained un-passivized. The refractive index, thickness, and reflectance of the films were measured using an optical reflectometer (Filmetrics F20) employing white light in a frequency range of 3×10^{14}–7.5×10^{14} Hz (using combinations of different wavelengths ranging from 400 nm to 1000 nm). The surface morphology was characterized using an atomic force microscope (Dimension Edge, Bruker). After making the contacts metallization and annealing, the photocurrent measurements before and after electron irradiation were made using a simulator (Leios IV SolarCT) under AM0 and white light illumination conditions. The *I–V* measurements were obtained immediately after the electron irradiation. Capacitance voltage (*C-V*) and dark *I-V* characteristics

were carried out by using semiconductor parameter analyzer (Keithley Model 4200-SCS). Solar cells were exposed to 9 MeV electrons (5.09×10^{16} e/cm^2) at room temperature using a linear accelerator (LINAC). The LINAC used in our experiment is a Siemens PRIMUS LINAC, installed in Mount Mirium cancer hospital Penang, Malaysia. It was used, keeping in view its best beam uniformity, symmetry and dose linearity (Reena et al., 2006).

Thermal annealing of irradiated solar cells was performed at 400 °C for 30 min After annealing the solar cells were reanalysed for *I-V*, *C-V*, and frequency dependent conductance (G_p) measurements.

3. Results and discussion

3.1. Surface morphology

The AFM images, typical surface morphology illustrated the height roughness (R_a) and root mean square roughness (rms). R_a and rms values are strongly influenced by the degree of accumulation and cluster size of the films (Raoufi et al., 2007). From Fig. 1 (a), height roughness (R_a) and root mean square roughness (rms) values of SiO_2 film were obtained to be 13.7 nm and 135 nm, respectively.

From Fig. 1(b), Ra and rms values of 13.1 nm and 118 nm were determined, respectively. The SiO_2 AR layer in the solar cells increased the light absorption in the visible region of the solar spectrum and increased the photo conversion process, thereby enhancing the efficiency of the Si solar cell (Ali et al., 2014). While in case of as-grown p-type (100) c-Si substrate R_a and rms were formed to be 0.092 nm and 2.86 nm, respectively. As-grown Si surface shows a very smooth surface with a few nanometer surface roughness. This indicates that the solar cells with ARC absorb more light as compared to the as-grown solar cell. Surface topography of Al-alloyed P^+ layer, formed on the rear side of the solar cell is shown in Fig. 1(d). The size of Al grains in Al-alloyed P^+ layer is uniform in some range with little variation on the surface. Different regions of AFM image actually show aluminum-alloyed distribution over the rear side of solar cell. The bare Si has a high refractive index and an average solar reflectance of about 35% (Ali et al., 2014; Mazur et al., 2013). Therefore reflection losses can be lowered significantly by using a suitable AR coating. Fig. 2 shows that an average reflectance of approximately 13.1% and 12.9% was obtained for solar cells with and without FSP, respectively. It was observed that the maximum reduction in light reflection was obtained in the blue and green (450–630 nm) regions of the visible light spectrum. However a slight increase in the reflection from 630 to 1000 nm was also observed. The enhancement in the reflection was due to the random distribution of the SiO_2 film particles and the decrease in roughness of the surface.

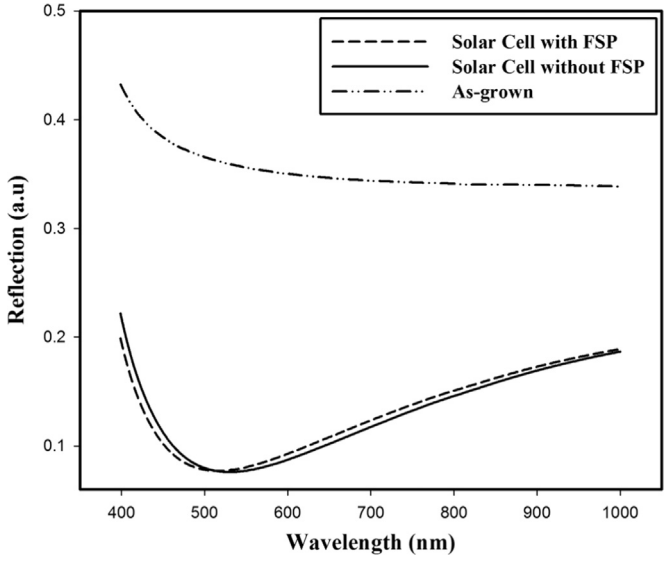

Fig. 2. Shows the reflectance of FSP and non-FSP solar cells with the as-grown Si substrate.

3.2. Capacitance-voltage measurements

By applying voltage *V*, the depletion layer capacitance per unit area was measured (Sze, 2007). The slope in $1/C^2$–V measures the carrier concentration (N_D) and can be measured by using following relationship (Faraz et al., 2010).

$$C = A\left[\frac{q\varepsilon_0\varepsilon_r N_D}{2(V_{bi} - V)}\right]^{1/2} \quad (1)$$

where *V* is positive/negative for forward/reverse bias, A is the area of the solar cell, N_D is the carrier concentration, q is the charge of the electron, ε_0 is the vacuum permittivity, ε_r is the dielectric constant of silicon, V_{bi} is the built-in potential. The depletion layer width (W_D) of the junction was obtained using the following general expression (Sze, 2007).

$$W_D = \frac{\varepsilon_0\varepsilon_r A}{C} \quad (2)$$

Fig. 3 shows that the measured depletion layer widths for the FSP solar cell before irradiation were 0.17 μm at zero bias and 1.16 μm at −2 V bias. While after electron irradiation, the depletion widths increased to 0.44 μm at zero bias and 1.31 μm at −2 V bias. Fig. 4 shows the measured depletion layer widths for the solar cell without FSP before and after electron irradiation. It was observed that before electron irradiation, the depletion layer widths were 0.43 μm at zero bias and 1.39 μm at −2.0 V bias while at 5.09×10^{16} e/cm^2 the depletion widths increased to 0.73 μm at zero bias and 1.51 μm at −2.0 V bias. Broadening of W_D was due to majority carriers trapping by the defects produced by electron irradiation. Fig. 4 also represents the dependence of $1/C^2$ on the applied voltage *V* of an electron irradiated silicon solar cell. It was observed that a linear relation exists at reverse voltages and its intercept with the voltage-axis is analogous to the depletion potential.

Effect of electron irradiation on the carrier concentration is shown in Fig. 5. It was observed that there is a slight reduction in the carrier concentration for FSP solar cell from 2.0×10^{15} cm^{-3} to

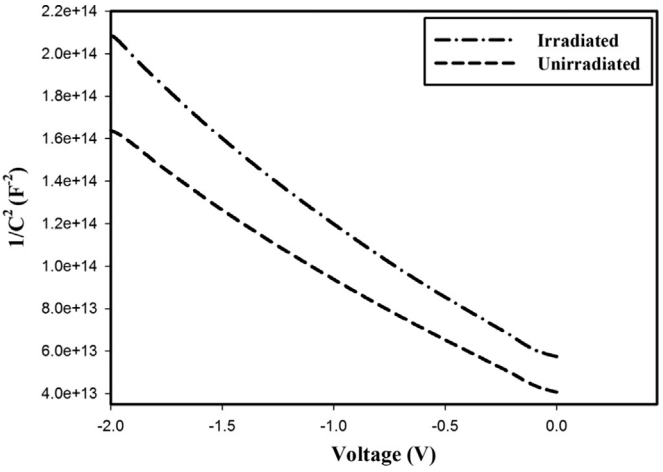

Fig. 3. Plot of $1/C^2$ versus voltage for c-Si solar cell with FSP.

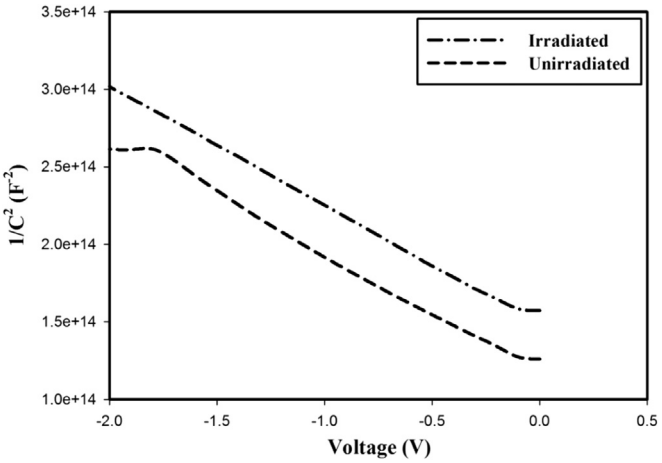

Fig. 4. Plot of $1/C^2$ versus voltage for c-Si solar cell without FSP.

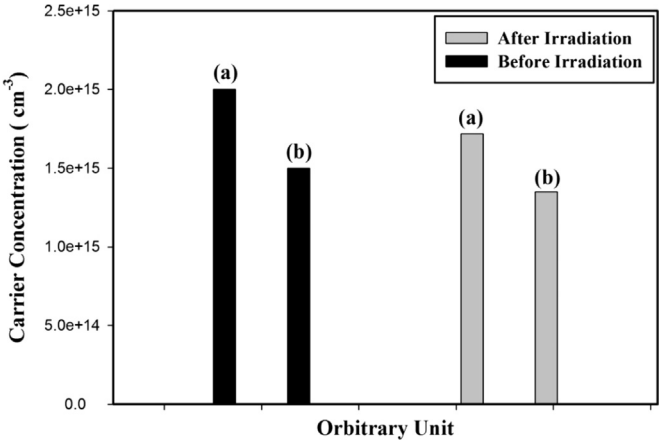

Fig. 5. Carrier concentration (a) solar cell with FSP (b) solar cell without FSP.

1.72×10^{15} cm^{-3} while in case of non-FSP solar cell, it decreased from 1.50×10^{15} cm^{-3} to 1.35×10^{15} cm^{-3} due to 9 MeV electron irradiation. The decrease in carrier concentration was due to the presence of radiation induced defects, which play a dominating role in charge carriers trapping or forming recombination centres (Summers et al., 1993). Frequency dependent conductance (G_P) techniques have been used to adequately investigate the interface trap states in the silicon solar cells. Applying this method, it is viable to extract the interface trap states density in the depletion and the weak inversion regions of the band gap (Chattopadhyay, 1996). From the maximum value of frequency versus G_p/ω plot, the interface state density and the interface trap time constant can be extracted (Hussain et al., 2012),

$$N_{ss} = \frac{2.5}{q}\left[\frac{G_p}{\omega}\right]_{max} \quad (3)$$

where q and G_p are the charge of the electron and the conductance respectively, while $\omega = 2\pi f$ is the angular frequency, f is the frequency. The maximum peak value in the plot of "frequency versus G_p/ω" is due to the presence of interface trap centres, which are present at the interfaces of the solar cells (Çakar et al., 2007). The effect of 9 MeV irradiation on the G_p/ω values measured from the calculated conductance values Vs frequency is shown in Figs. 6 and 7.

The interface trap density for the solar cell with FSP realized before irradiation was 1.21×10^{12} eV^{-1} cm^{-2} and increased to 1.65×10^{12} eV^{-1} cm^{-2} after the electron irradiation. While the interface trap density for the solar cell without FSP realized

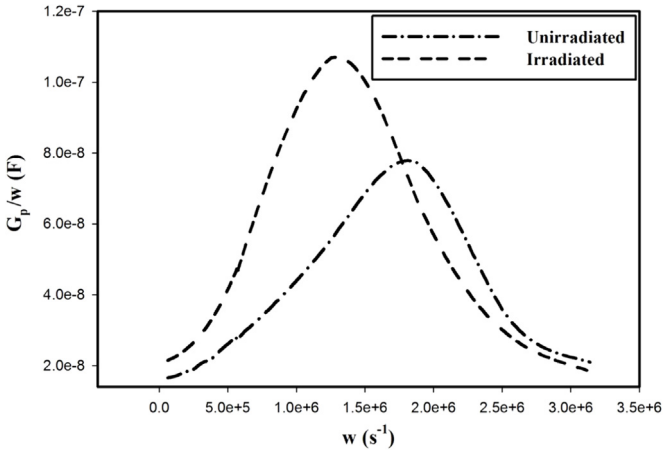

Fig. 6. G_p/ω vs. frequency characteristics for c-Si solar cell with FSP.

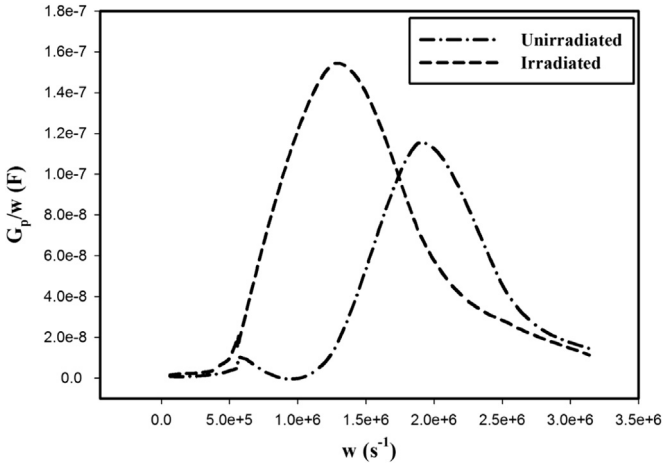

Fig. 7. G_p/ω vs. frequency characteristics for c-Si solar cell without FSP.

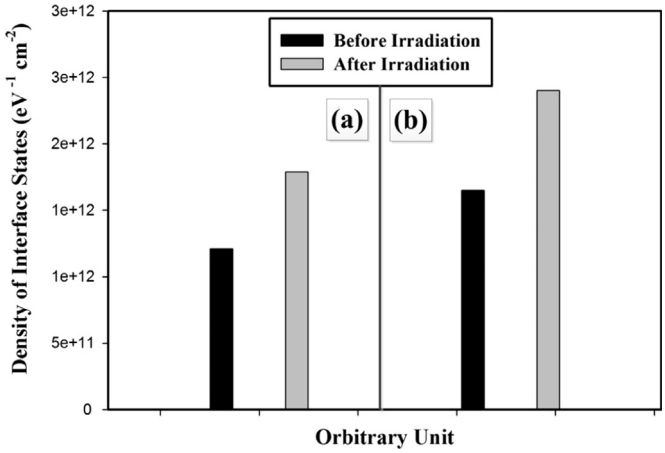

Fig. 8. Density of interface states (a) solar cell with FSP (b) solar cell without FSP.

increased from 1.79×10^{12} eV^{-1} cm^{-2} to 2.40×10^{12} eV^{-1} cm^{-2} before and after the electron irradiation, respectively. FSP solar cell presented low values of interface state density as compared to non-FSP solar cell for both pre and post irradiation. Fig. 8 shows the interface state density value before and after electron irradiation for both types of solar cells. This phenomenon can be explained as the electron passes through the solar cell material, the energy dissipation of electron displaces the atoms in the lattice and thus the defects or trap levels are generated. These trap

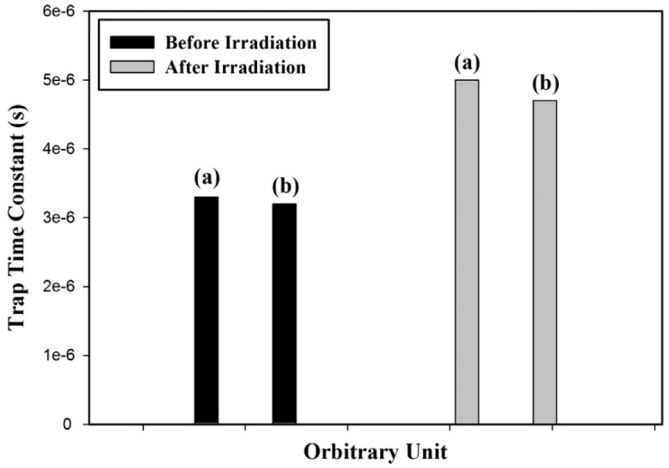

Fig. 9. Trap time constant (a) solar cell with FSP (b) solar cell without FSP.

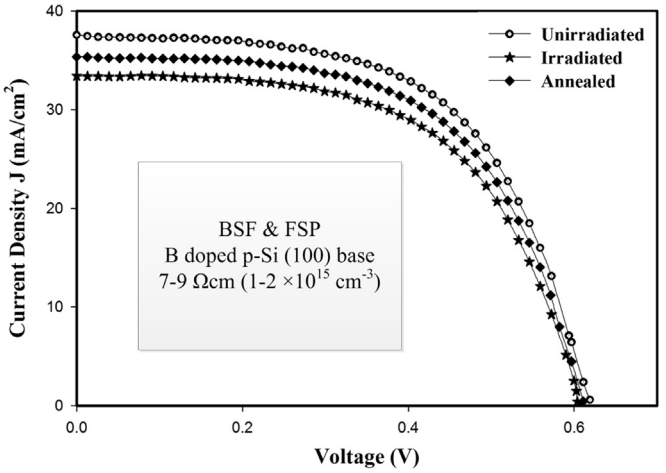

Fig. 10. Current–Voltage measurements of pre and post-irradiation and annealed solar cell.

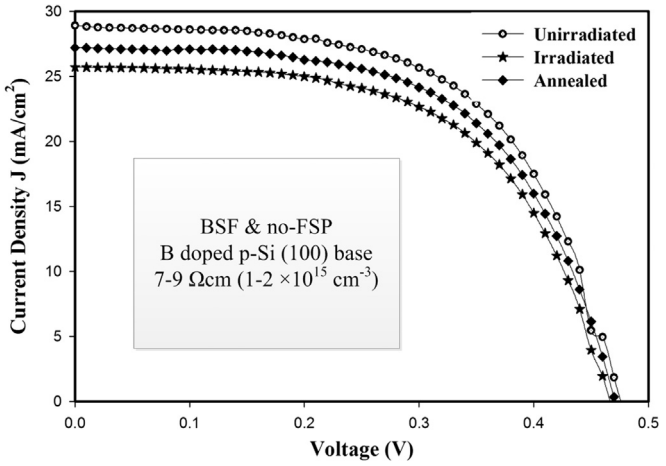

Fig. 11. Current–Voltage measurements of pre and post irradiation and annealed solar cell.

centres could be passive or active, but mostly these defects are electrically active which affect the carrier concentration by trapping the charge carriers (Srivastava et al., 2006).

Also the trap times for the charging and discharging of trap levels can be calculated by analyzing of the solar cells at different frequencies. The Fermi level plays an important role in the analysis of interface trap centres. At a particular bias the occupancy of this interface trap centres is fixed by the Fermi level. Moreover, it helps in determining the time constant of the related interface trap levels at the Si surface with a specific interface charge density.

It was observed that for the solar cell with FSP there was an increase in the trap time constant from 3.3×10^{-6} s to 5×10^{-6} s while the solar cell without FSP shows an increase in trap time constant from 3.2×10^{-6} s to 4.7×10^{-6} s after electron irradiation. Fig. 9 describes that the enhancement in the trap time constant is an evidence that the free carriers (that actually can take part in conduction process) decrease with irradiation. This phenomenon might be attributed to the longer capture time for radiation induced defect centres corresponding to the charge transfer rate for the centres to efficiently trap the carriers (Miller et al., 2000).

The conversion efficiency (η) is an important parameter and it can be extracted from the following relationship (Fonash, 2012),

$$\eta = \frac{I_{SC} V_{OC} FF}{P_{in}} \tag{4}$$

where I_{sc} is the short circuit current, V_{oc} is the open circuit voltage and P_{in} is the incident light power. A significant improvement in the open-circuit voltage and the overall efficiency was observed as compared to solar cell without FSP (Figs. 10 and 11). This enhancement in solar cell efficiency can be attributed to the lower surface recombination velocity of charge carriers (Green, 1990, 1987). Fine passivation layer helps in reducing the dangling bonds formed on the emitter surface region due to high temperature treatment of the solar cells (Green, 1987). However, the short circuit current was not affected much due to the formation of intentional passivation layer.

The *I-V* characteristics of the unirradiated and irradiated FSP solar cell are shown in Fig. 10. The solar cell efficiency was degraded after electron irradiation. It was noticed that the short circuit current decreased slight rapidly as compared to the open circuit voltage. Table 1 summarizes the device performance of the pre and post irradiated solar cell. The solar cell without electron irradiation has shown the V_{oc} of 619 mV which decreases by ΔV_{oc}=13 mV for the irradiated solar cell. This results in the degradation of cell efficiency to 11.7%, which is a decrease of 1.5% absolute in comparison to the unirradiated solar cell. Efficiencies have been quoted to one decimal digit while the current/voltages have been mentioned with three digits (Cuevas et al., 1999; Juvonen et al., 2002).

Table 1
Current–Voltage measurements of pre and post irradiation and annealed solar cell.

Treatment	V_{oc} (mV)	J_{sc} (mA)	V_m (mV)	J_m (mA)	η (%)	η_{deg} (%)	η_{rec} (%)
Unirradiated	619	37.6	450	29.9	13.2	–	–
Irradiated	606	33.4	433	27.3	11.7	11.3	–
Annealed	610	35.2	443	28.6	12.6	–	95

Table 2
Current–Voltage measurements of pre and post irradiation and annealed solar cell.

Treatment	V_{oc} (mV)	J_{sc} (mA)	V_m (mV)	J_m (mA)	η (%)	η_{deg} (%)	η_{rec} (%)
Unirradiated	473	28.9	315	24.7	7.8	–	–
Irradiated	465	25.6	289	22.9	6.6	15.3	–
Annealed	469	27.1	302	23.9	7.1	–	91

Fig. 11 shows that the short circuit current decreases more rapidly as compared to the open circuit voltage. From the data given in Table 2, the solar cell without electron irradiation has shown the V_{oc} of 473 mV which decreases by ΔV_{oc}=8 mV for the irradiated solar cell. This results in the degradation of cell efficiency to 6.6%, which is a decrease of 1.2% absolute in comparison to the

unirradiated solar cell.

3.3. Effect of thermal annealing on electron irradiated c-Si solar cell

The electron irradiated solar cell was thermally annealed in nitrogen atmosphere at 400 °C for 1800s The initial efficiency can be restored by annealing the solar cell for various time duration. But the restoration depends on the radiation fluence and radiation resistant properties of the solar cell (Khan et al., 2002a; Kuendig and Shah, 2002). The data given in Table 1 represents that the annealed solar cell without FSP has shown an open circuit voltage V_{oc} of 610 mV which increases by $\Delta V_{oc}=4$ mV as compared to the irradiated solar cell. On the other hand the annealed solar cell has shown J_{sc} of 35.2 mA which increases by $\Delta J_{sc}=1.8$ mA as compared to the irradiated solar cell. The results indicate that there was 95% recovery in the efficiency as compared to the unirradiated solar cell. Results were interpreted as compared to previous work and good result were achieved in comparison to the existing work (Horiuchi et al., 2000; Khan et al., 2002b).

The data given in Table 2 represents that the annealed FSP solar cell has shown an open circuit voltage V_{oc} of 469 mV which increases by $\Delta V_{oc}=4$ mV as compared to the irradiated solar cell. On the other hand the annealed solar cell has shown J_{sc} of 27.1 mA which increases by $\Delta J_{sc}=1.5$ mA as compared to the irradiated solar cell. Efficiencies have been quoted to one decimal digit while the current/voltages have been mentioned with three digits (Green et al., 1984). The results indicate that the annealing process has initiated 91% restoration in the efficiency as compared to the unirradiated solar cell. The above results confirm that the BSF-FSP solar cell with ARC was more resistant to radiation than its counterpart. The BSF-FSP solar cell shows lowest efficiency degradation ratio and comparatively showed better results for crystalline solar cell (Ryu et al., 2008). Further the BSF-FSP solar cell showed better results in view of short circuit current, fill factor, open circuit voltage and radiation degradation when compared to previous work (Ashry and Fares, 2012).

Annealing process actually involves in the passivation of the irradiation induced defects of the solar cell. The *J-V* results depict that the overall performance of electron irradiated solar cell has been improved after annealing process (Horiuchi et al., 2000). Corresponding to these outcomes, the enhancement in the efficiency of the annealed Si solar cell is primarily attributed to the annealing process which dissociates and annihilates the metastable clusters of vacancies that stays at the interstitial sites (Newman, 1982). The annealing process conditions significantly affect the annihilation of defects.

4. Conclusion

The c-Si solar cells were fabricated with and without FSP and characterized for their radiation tolerance at fluence of 5.09×10^{16} e/cm^2. Different parameters such as the current-voltage, carrier concentration, depletion layer width, density of interface states, and the trap time constant have been studied systematically with the following conclusions:

- Capacitance-Voltage measurements represent that there is a slight decrease in the carrier concentration (N_D) and little increase in depletion layer width (W_D). This investigation depicts the presence of radiation induced defects, which play a dominating role in forming the recombination centres.
- A small increase in the density of interface states (N_{ss}) and trap time constant (τ) was observed from the conductance–frequency measurements. This phenomenon represents that after electron irradiation, the trap levels are generated. These levels trap the charge carriers and thus the trap time constant is increased. It is due to the fact that the capture time for radiation induced defect centres were long enough compared to the charge transfer rate.
- The *J-V* measurements depict that the conversion efficiencies of FSP and non-FSP solar cells were decreased by 1.5% and 1.2% absolute after irradiation, respectively. FSP solar cell presented low efficiency degradation ratio of 11.3% as compared to 15.3% of the solar cell without FSP.
- The thermal recovery of irradiated solar cells indicate that FSP solar cell has better radiation tolerance. Further, the radiation damage was restored to the extent obtained before radiation. Based on these results, optimized BSF-FSP solar cell presents its potential in the production of low-cost, radiation resistant Si solar cells.

Acknowledgement

The authors acknowledge the Short Term Research Grant Scheme (1001/PFIZIK/845015) and Universiti Sains Malaysia (USM) for the Fellowship to Khuram Ali.

References

Ali, K., Khan, S.A., MatJafri, M., 2013. ^{60}Co γ-irradiation effects on electrical characteristics of monocrystalline silicon solar cell. Int. J. Electrochem. Sci. 8, 7831–7841.
Ali, K., Khan, S.A., Mat Jafri, M.Z., 2014. Enhancement of silicon solar cell efficiency by using back surface field in comparison of different antireflective coatings. Sol. Energy 101, 1–7.
Ashry, M., Fares, S., 2012. Electrical characteristic measurement of the fabricated CdSe/P-Si heterojunction solar cell under radiation effect. Microelectron. Solid State Electron. 1, 41–46.
Bourgoin, J., De Angelis, N., 2001. Radiation-induced defects in solar cell materials. Sol. Energy Mater. Sol. Cells 66, 467–477.
Çakar, M., Yıldırım, N., Doğan, H., Türüt, A., 2007. The conductance and capacitance–frequency characteristics of Au/pyronine-B/p-type Si/Al contacts. Appl. Surf. Sci. 253, 3464–3468.
Chattopadhyay, P., 1996. Capacitance technique for the determination of interface state density of metal-semiconductor contact. Solid-State Electron. 39, 1491–1493.
Corbett, J.W., 1966. Solid State Physics, Suppl. 7: Electron Radiation Damage in Semiconductors and Metals, Academic Press.
Cuevas, A., Stocks, M., McDonald, D., Kerr, M., Samundsett, C., 1999. Samundsett, Recombination and trapping in multicrystalline silicon. IEEE Trans. Electron Dev. 46, 2026–2034.
Faraz, S.M., Ashraf, H., Arshad, M.I., Hageman, P.R., Asghar, M., Wahab, Q., 2010. Interface state density of free-standing GaN Schottky diodes. Semicond. Sci. Technol. 25, 095008.
Fonash, S., 2012. Solar Cell Device Physics. Elsevier, Academic Press, INC (London), Ltd.
Green, M.A., 1990. Intrinsic concentration, effective densities of states, and effective mass in silicon. J. Appl. Phys. 67, 2944–2954.
Green, M.A., Blakers, A.W., Shi, J., Keller, E.M., Wenham, S.R., 1984. High-efficiency silicon solar cells. IEEE Trans. Electron Dev. 31, 679–683.
Green, M.A. High Efficiency Silicon Solar Cells, Hardcover ed., 1987.
Horiuchi, N., Nozaki, T., Chiba, A., 2000. Improvement in electrical performance of radiation-damaged silicon solar cells by annealing. Nucl. Instrum. Methods in Phys. Res. Sect. A: Accel. Spectrom. Detect. Assoc. Equip. 443, 186–193.
Hu, Z., He, S., Yang, D., 2006. Radiation effects of protons and electrons on backfield silicon solar cells. In: Protection of Materials and Structures from the Space Environment, Springer, pp. 1–8.
Hussain, I., Soomro, M.Y., Bano, N., Nur, O., Willander, M., 2012. Interface trap characterization and electrical properties of Au-ZnO nanorod Schottky diodes by conductance and capacitance methods. J. Appl. Phys. 112.
Juvonen, T., Härkönen, J., Kuivalainen, P., 2002. High efficiency single crystalline silicon solar cells. Phys. Scr. 2002, 96.
Kao, W., Ali, A., Hwang, E., Mookerjea, S., Datta, S., 2010. Effect of interface states on sub-threshold response of III–V MOSFETs, MOS HEMTs and tunnel FETs. Solid-State Electron. 54, 1665–1668.
Kawasuso, A., Hasegawa, M., Suezawa, M., Yamaguchi, S., Sumino, K., 1995. An annealing study of defects induced by electron irradiation of Czochralski-grown Si using a positron lifetime technique. Appl. Surf. Sci. 85, 280–286.
Khan, A., Yamaguchi, M., Bourgoin, J.C., Takamoto, T., 2002a. Thermal annealing study of 1 MeV electron-irradiation-induced defects in n+p InGaP diodes and

solar cells. J. Appl. Phys. 91, 2391–2397.
Khan, A., Yamaguchi, M., Bourgoin, J.C., Takamoto, T., 2002b. Thermal annealing study of 1 MeV electron-irradiation-induced defects in n+p InGaP diodes and solar cells. J. Appl. Phys. 91, 2391–2397.
Kuendig, J., Shah, A, 2002. Effect of proton irradiation and subsequent thermal annealing on the characteristics of thin-film silicon solar cells and microcrystalline silicon layers. In: Photovoltaic Specialists Conference, 2002. Conference Record of the Twenty-Ninth IEEE, 2002, pp. 974–977.
Mazur, M., Wojcieszak, D., Domaradzki, J., Kaczmarek, D., Song, S., Placido, F., 2013. TiO_2/SiO_2 multilayer as an antireflective and protective coating deposited by microwave assisted magnetron sputtering. Opto-Electron. Rev. 21, 233–238.
Miller, E.J., Dang, X.Z., Wieder, H.H., Asbeck, P.M., Yu, E.T., Sullivan, G.J., Redwing, J. M., 2000. Trap characterization by gate-drain conductance and capacitance dispersion studies of an AlGaN/GaN heterostructure field-effect transistor. J. Appl. Phys. 87, 8070–8073.
Newman, R.C., 1982. Defects in silicon. Rep. Progress. Phys. 45, 1163.
Ng, Kwok K., Sze, S.M., 2007. Physics of Semiconductor Devices, Third ed. John Wiley and Sons, New Delhi.
Nicollian, E.H., Brews, J.R., 1982. MOS (Metal Oxide Semiconductor) Physics and Technology. Wiley, New York.
Rao, A., Krishnan, S., Sanjeev, G., Siddappa, K., 2009. Effect of 8 MeV electrons on Au/n-Si Schottky diodes. Int. J. Pure Appl. Phys. 5, 55–62.
Raoufi, D., Kiasatpour, A., Fallah, H.R., Rozatian, A.S.H., 2007. Surface characterization and microstructure of ITO thin films at different annealing temperatures. Appl. Surf. Sci. 253, 9085–9090.
Reena, P., Dayananda, S., Pai, R., Jamema, S.V., Gupta, T., Deepak, D., Rajeev, S., 2006. Performance characterization of siemens primus linear accelerator under small monitor unit and small segments for the implementation of step-and-shoot intensity-modulated radiotherapy. J. Med. Phys. 31, 269–274.
Ryu, K., Kim, H., Min, K, 2008. Radiation Effect Test for Single-Crystalline and Polycrystalline Silicon Solar Cells.
Sathyanarayana Bhat, P., Rao, A., Krishnan, S., Sanjeev, G., Puthanveettil, S.E., 2014. A study on the variation of c-Si solar cell parameters under 8 MeV electron irradiation. Sol. Energy Mater. Sol. Cells 120, 191–196.
Sathyanarayana Bhat, P., Rao, A., Sanjeev, G., Usha, G., Priya, G.K., Sankaran, M., Puthanveettil, S.E., 2015. Capacitance and conductance studies on silicon solar cells subjected to 8 MeV electron irradiations. Radiat. Phys. Chem. 111, 28–35.
Srivastava, P.C., Pandey, S.P., Asokan, K., 2006. A study on swift (~100 MeV) heavy (Si8+) ion irradiated crystalline Si-solar cell. Nucl. Instrum. Methods Phys. Res. Sect. B: Beam Interact. Mater. At. 244, 166–170.
Srour, J., Marshall, C.J., Marshall, P.W., 2003. Review of displacement damage effects in silicon devices. IEEE Trans. Nucl. Sci. 50, 653–670.
Summers, G.P., Burke, E.A., Shapiro, P., Messenger, S.R., Walters, R.J., 1993. Damage correlations in semiconductors exposed to gamma, electron and proton radiations. IEEE Trans. Nucl. Sci. 40, 1372–1379.
Yamaguchi, M., 2001. Radiation-resistant solar cells for space use. Sol. Energy Mater. Sol. Cells 68, 31–53.
Yamaguchi, M., Itoh, Y., Ando, K., 1984. Room-temperature annealing of radiation-induced defects in InP solar cells. Appl. Phys. Lett. 45, 1206–1208.